Transactions of the VŠB – Technical University of Ostrava, Mechanical Series
No. 2, 2014, vol. LX
article No. 1990

Dawid PIETRALA[*], Paweł ŁASKI[**]

KINEMATIC ANALYSIS 6DOF DELTA MANIPULATOR

KINEMATICKÁ ANALÝZA DELTA MANIPULÁTORU SE 6DOF

Abstract

In the paper the solid and kinematic model of delta type parallel manipulator with six degrees of freedom is proposed. Method of determining the manipulator kinematics equations using the notation of Denavitt – Hartenberg is presented. For given movements of manipulator platform the trajectory of drives are illustrated. Also working space for various platform orientations are showed.

Abstrakt

V článku je popsán model mechanické struktury a model pro kinematickou analýzu paralelního manipulátoru typu delta se 6 stupni volnosti. Kinematický model manipulátoru je sestaven s využitím Denavitt – Hartenbergova principu. Pro požadovanou trajektorii koncové platformy manipulátoru byly vygenerovány průběhy poloh jednotlivých pohonů. Dále byl vyšetřen pracovní prostor manipulátoru pro možné orientace koncové platformy.

Keywords

Parallel manipulator, kinematic analysis, degrees of freedom, inverse kinematic, forward kinematic.

1 INTRODUCTION

Industrial manipulators is now one of the main elements of flexible manufacturing systems. These devices can be divided into two basic groups: manipulators with open kinematic chain and manipulators with a closed kinematic chain. Regardless of the construction of the manipulator for each device kinematic model needs to be developed. This issue is essential for control of the manipulator. It allows during the development stages determine the performance characteristics of drives and manipulator workspace.

The simple task of serial manipulators kinematics has a unique solution. In contrast, inverse kinematics is ambiguous and has frequently so many solutions as a degree of freedom manipulator. In parallel manipulators these issues are much more difficult to analyze. This article shows how to determine the kinematic model of parallel manipulator with six degrees of freedom. This article shows how to solve the simple and inverse kinematics task and presents the results of simulation studies carried out on the kinematic model.

[*] Titles, Department of Automation and Robotics, Faculty of Mechatronics and Mechanical Engineering, Kielce University of Technology, al. Tysiąclecia P. P. 7, Kielce, tel. (+48) 788 146 391, dpietrala@tu.kielce.pl
[**] Titles, Department of Automation and Robotics, Faculty of Mechatronics and Mechanical Engineering, Kielce University of Technology, al. Tysiąclecia P. P. 7, Kielce, tel. (+48) 603 422 492, pawell@tu.kielce.pl

2 KINEMATIC ANALYSIS

The presented manipulator (Fig 1) is constructed of the fixed base, six identical and independent moving arms and work platform. Each arm consists of an active and passive parts of the two spherical joints. The manipulator has six degrees of freedom. The mobility of the manipulator determined from the formula (1). Kinematic diagram of the manipulator shown in fig 1. *R* means rotatable joint, and *S* spherical joint.

$$\begin{aligned} w &= 6(n-1) - \sum_{i=1}^{5} ip_i \\ w &= 6 \cdot 13 - 6 \cdot 5 - 6 \cdot 3 - 6 \cdot 4 \\ w &= 6 \end{aligned} \tag{1}$$

where:

w - manipulator mobility,

n - the number of mobile manipulator members,

i - kinematic pairs of the given class,

p_i - the class of the given kinematic pair.

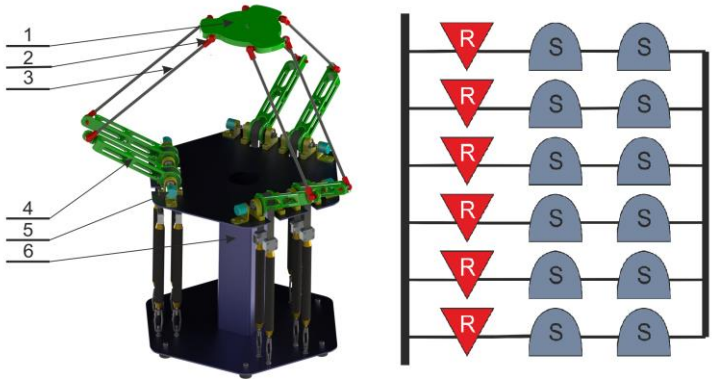

Fig 1 Solid model of manipulator: 1 – working platform, 2 – spherical joint, 3 – passive arm, 4 active arm, 5 – drive unit, 6 – base.

The kinematic model of manipulator is a mathematical relations between the coordinates of the drive configuration and effector Cartesian coordinates. Simple kinematics task consists in determining the coordinates of the position and orientation of the effector, knowing the actual drive configuration coordinates. Inverse kinematics consists in determining the coordinates of the drive configuration, knowing a predetermined position and orientation of the platform. In order to determine the kinematic model of manipulator must first determine how is defined the position and orientation of the working platform. With basis of manipulator the Cartesian coordinate system U_0 is linked and with working platform is connected Cartesian coordinate system UP. Position coordinates of the work platform is $P_{x,y,z}$ of the beginning of UP with respect to the basic coordinate system U_0 (fig 2).

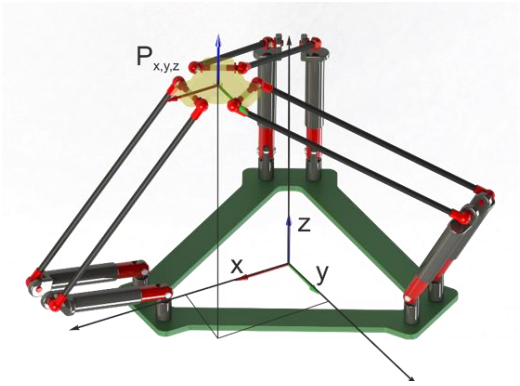

Fig 2 Pozycja platform roboczej

Orientation of the work platform is uniquely defined as a matrix of nine directional cosine of the coordinate system UP relative to the base coordinate system U_0. This method of determining the orientation is very inconvenient for the user of manipulator. Therefore it is assumed that the orientation is defined as the three angles of rotation α, β, γ around the axis of the current coordinate system UP. Because the order of rotation is important convention was adopted that the angle is the angle of rotation around the axis x_1. This rotation creates a new coordinate system. The angle β is the angle of rotation around the axis y_2 and this rotation creates a new coordinate system. The angle γ is the angle of rotation around the axis z_3. The end result is the coordinate system that defines the orientation of the work platform (fig 3). Matrix that defines the position and orientation of the work platform (2) was established due to make a shift along the axis of the base coordinate system and three rotations around the axis of the associated current platform coordinate system.

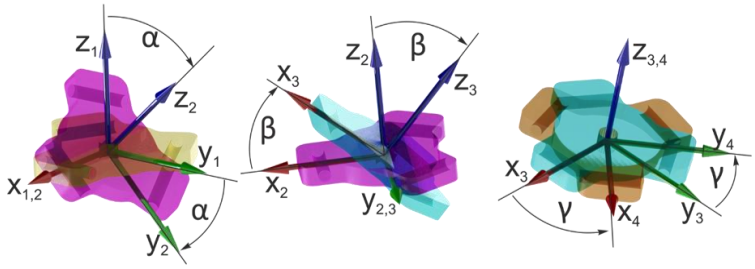

Fig 3 Working platform orientation

$$M_{zad} = \begin{bmatrix} R_{zad} & P_{zad} \\ 0 & 1 \end{bmatrix} \tag{2}$$

All manipulator arms have the same structure, therefore determination of the kinematic model is presented on the example of one arm. Each movable arm member is bound to the coordinate system $UR_{i,j}$, where *i* – arm number, *j* – coordinate system number of i –th arm. Coordinate system $UR_{i,j}$ was created by transforming the previous system ($UR_{i,j-1}$). For each coordinates system the transformation matrix was determined which is defining the position and orientation relative to the previous system. Systems $UR_{i,1} - UR_{i,3}$ shown in fig 4. and the corresponding transformation matrices is described by the equation (3).

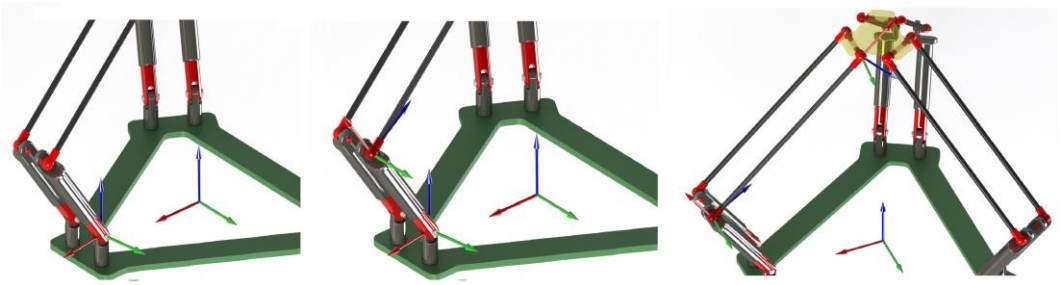

Fig 4 Location of systems $UR_{i,1}, UR_{i,2}, UR_{i,3}$

$$M_{i,0}^{i,1} = \begin{bmatrix} \cos(\xi_i) & -\sin(\xi_i) & 0 & R\cos(\xi_i) \\ \sin(\xi_i) & \cos(\xi_i) & 0 & R\sin(\xi_i) \\ 0 & 0 & 1 & H \\ 0 & 0 & 0 & 1 \end{bmatrix}$$

$$M_{i,1}^{i,2} = \begin{bmatrix} \cos(\theta_{i,1})\cos(\pm\xi_0) & -\sin(\pm\xi_0) & \sin(\theta_{i,1})\sin(\pm\xi_0) & l_1\cos(\theta_{i,1})\cos(\pm\xi_0) \\ \cos(\theta_{i,1})\sin(\pm\xi_0) & \cos(\pm\xi_0) & \sin(\theta_{i,1})\sin(\pm\xi_0) & l_1\cos(\theta_{i,1})\sin(\pm\xi_0) \\ -\sin(\theta_{i,1}) & 0 & \cos(\theta_{i,1}) & -l_1\sin(\theta_{i,1}) \\ 0 & 0 & 0 & 1 \end{bmatrix} \quad (3)$$

$$M_{i,2}^{i,3} = \begin{bmatrix} \cos(\theta_{i,2})\cos(\theta_{i,3}) & -\cos(\theta_{i,2})\sin(\theta_{i,3}) & \sin(\theta_{i,2}) & l_2\cos(\theta_{i,2})\cos(\theta_{i,3}) \\ \sin(\theta_{i,3}) & \cos(\theta_{i,3}) & 0 & l_2\sin(\theta_{i,3}) \\ -\cos(\theta_{i,3})\sin(\theta_{i,2}) & \sin(\theta_{i,2})\sin(\theta_{i,3}) & \cos(\theta_{i,2}) & -l_2\sin(\theta_{i,2})\cos(\theta_{i,3}) \\ 0 & 0 & 0 & 1 \end{bmatrix}$$

where:

R - radius of the circle on which base are arranged arms,

l_1, l_2 - length of active and passive arm,

H - distance along the axis Z from begining of system U_0 to the beginning of the $UR_{i,1}$.

Then, using the Euler angles transformed system $UR_{i,3}$ to system UP. The location of these systems are shown in fig 5. The transformation matrix is described by the equation (4).

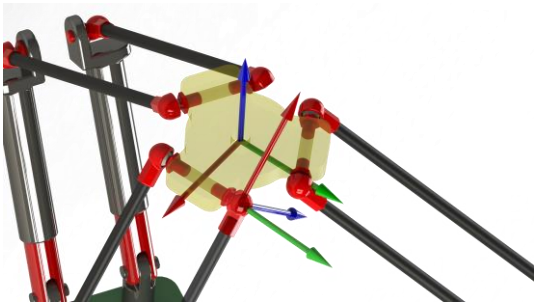

Fig 5 Location of coordination systems $UR_{i,3}, UP$

$$M_{i,3}^{i,4}=\begin{bmatrix}\cos(\theta_{i,4})\cos(\theta_{i,6})-\sin(\theta_{i,4})\cos(\theta_{i,5})\sin(\theta_{i,6}) & \sin(\theta_{i,4})(-\cos(\theta_{i,5}))\cos(\theta_{i,6})-\cos(\theta_{i,4})\sin(\theta_{i,6}) & \sin(\theta_{i,4})\sin(\theta_{i,5}) & 0\\ \cos(\theta_{i,4})\cos(\theta_{i,5})\sin(\theta_{i,6})+\sin(\theta_{i,4})\cos(\theta_{i,6}) & \cos(\theta_{i,4})\cos(\theta_{i,5})\cos(\theta_{i,6})-\sin(\theta_{i,4})\sin(\theta_{i,6}) & -\cos(\theta_{i,4})\sin(\theta_{i,5}) & 0\\ \sin(\theta_{i,5})\sin(\theta_{i,6}) & \sin(\theta_{i,5})\cos(\theta_{i,6}) & \cos(\theta_{i,5}) & 0\\ 0 & 0 & 0 & 1\end{bmatrix} \quad (4)$$

Multiplying by the formula (5) previously designated matrices we obtain the final matrix $M_{i,0}^{i,4}$. This matrix defines the position and orientation of the working platform in the base coordinate system, it consist in sixteen elements. Submatrix *R* is a nine direction cosine matrix while the vector *P* determines the position of the working platform. All these elements are functions of the six variables which are configuration coordinates of the arm.

$$M_{i,0}^{i,4}(\theta_{i,\mathrm{j}})=M_{i,0}^{i,1}\cdot M_{i,1}^{i,2}\cdot M_{i,2}^{i,3}\cdot M_{i,3}^{i,4};i,\mathrm{j}=1,2,...,6$$
$$M_{i,0}^{i,4}=\begin{bmatrix}R & P\\ 0 & 1\end{bmatrix}=\begin{bmatrix}R_{x_4x_0} & R_{y_{46}x_0} & R_{z_4x_0} & P_{x_4}\\ R_{x_4y_0} & R_{y_4y_0} & R_{z_4y_0} & P_{y_4}\\ R_{x_4z_0} & R_{y_4z_0} & R_{z_4z_0} & P_{z_4}\\ 0 & 0 & 0 & 1\end{bmatrix} \quad (5)$$

In order to solve the inverse kinematics for each arm according to the formula (6) the system of six equations with six unknowns was established. With the previously fixed matrix (5) Six elements were selected and aligned to corresponding matrix elements set (2). The system is solved using the Newton-Raphson method. In this manner, six figures $\theta_{i,\mathrm{j}};\mathrm{j}=1,2,...,6$ which are the configuration coordinates i – th arm. Coordinate $\theta_{i,1}$ is the drive coordinate.

$$U_i=\begin{Bmatrix}P_{i,x_4}-x=0\\ P_{i,y_4}-y=0\\ P_{i,z_4}-z=0\\ R_{i,x_4x_0}-R_{xx}=0\\ R_{i,y_4y_0}-R_{yy}=0\\ R_{i,z_4z_0}-R_{zz}=0\end{Bmatrix} \quad (6)$$

The establishment of the six equations for one arm does not solve the task simple kinematics, because it is not known matrix (2) defining the position and orientation of the working platform but drive configuration coordinates are known. Thus, for each arm, five of the six coordinate remains unknown. An array of thirty equations with thirty unknowns was created according to the formula (7) . Since the individual elements of the matrix for all the arms are equal, likened them relative to each other. The thus-formed system were solved by the Newton-Raphson method. The result obtained thirty numbers $\theta_{i,\mathrm{j}};\mathrm{i}=1,2,...,6;\mathrm{j}=2,3,...,6$ which are configuration coordinates of all arms. Then, such calculated coordinates for i – th arm were substituted for the matrix $M_{i,0}^{i,4}$ (5). The values of individual elements of the matrix was determined. These values define the position and orientation of the working platform.

$$U=\begin{Bmatrix} P_{1,x_4}-P_{2,x_4}=0 \\ P_{1,y_4}-P_{2,y_4}=0 \\ P_{1,z_4}-P_{2,z_4}=0 \\ P_{1,x_4}-P_{3,x_4}=0 \\ \vdots \\ P_{5,z_4}-P_{6,z_4}=0 \end{Bmatrix} \tag{7}$$

On the created kinematic model of manipulator simulation studies was performed. For this purpose geometrical dimensions of manipulator was assumed: $R=500; l_1=400; l_2=700; H=100; [mm]$. For given position trajectory of work platform the configuration coordinate trajectories were designated. Were generated trajectories of circle on the plane X,Y at a constant value Z and for the fixed orientation of the working platform (8). For such a trajectory was determined drive waveforms shown in fig 6.

$$\begin{aligned} x(t)&=100cos(t); \\ y(t)&=100sin(t); \\ z(t)&=900; \end{aligned} \tag{8}$$

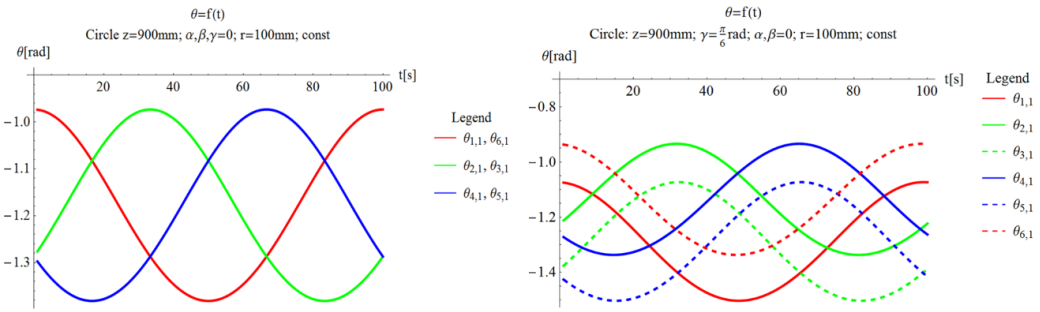

Fig 6 Waveforms of drives for a circle trajectory for two different orientations working platform.

Then the helix trajectory were generated for constant orientation of working platform which are described by the equation (9). For such a trajectory, waveforms of drives shown in fig 7. was determined.

$$\begin{aligned} x(t)&=100cos(t); \\ y(t)&=100sin(t); \\ z(t)&=900-3t; \end{aligned} \tag{9}$$

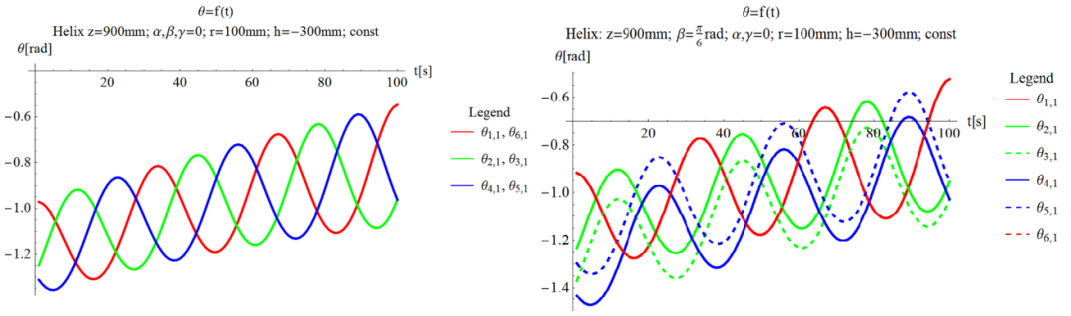

Fig 7 Waveforms of drives for helix trajectory for two different orientations of the working platform.

With kinematic model also manipulator workspace were determined. By working space should be understood set of points in space that is able to achieve an effector of manipulator at a constant predetermined orientation. The working space was determined using the simple task of kinematics. It was assumed restrictions on angle of drives $0 \div \frac{\pi}{2} rad$, and the range of motion of spherical joints $0 \div \frac{\pi}{2} rad; -\frac{\pi}{6} rad \div \frac{\pi}{6} rad$. fig 8 shows the working space for zero orientation ($\alpha, \beta, \gamma = 0$). Working space is determined with effector facing down. This configuration is the most common in industrial applications of parallel manipulators. The space is presented as an axonometric view, and views on different planes of the coordinate system.

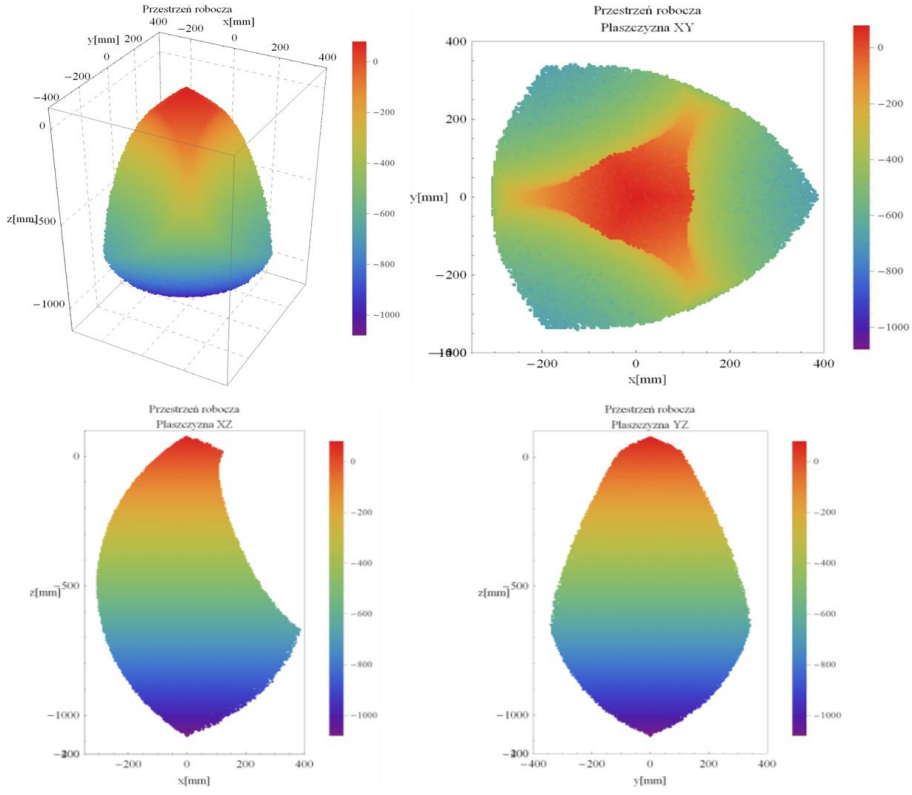

Fig 8 Manipulator working space.

3 SUMMARY

Manipulators with a closed kinematic chain is characterized by high stiffness and greater load capacity than serial manipulators. These devices are, however, difficult to control. Kinematic models of parallel manipulators are more complex than the models of serial manipulators and their solving requires from control system much more computing power. In addition, these manipulators have smaller workspaces in relation to serial manipulators with similar geometrical dimensions.

REFERENCES

[1] Tsai L.W. (1999) Robot Analysis: The Mechanics of Serial and Parallel Manipulators. John Wiley & Sons, New York

[2] Pietrala D. (2012) Projekt manipulatora o zamkniętym łańcuchu kinematycznym, o sześciu stopniach swobody z napędem elektrycznym. Innowacyjne rozwiązania w obszarze automatyki, robotyki i pomiarów, praca zbiorowa pod redakcją Janusza Kacprzyka, Warszawa 2013.

[3] Merlet J. P. (2000), Parallel robot, Springer, Verlag, New York, London.

[4] Farana Radim, Raiski M., Jezikova J.: Web based enterprise performance appraisal information system, International Conference on Engineering Education; 2010, pp.6

[5] J.E. Takosoglu, P.A. Laski, S. Blasiak, A fuzzy logic controller for the positioning control of an electro-pneumatic servo-drive, Proceedings of the Institution of Mechanical Engineers, Part I: Journal of Systems and Control Engineering 226 (2012) 1335–1343.

[6] Farana R, Licev L, Skuta J et al. (2009) 3-D Picturing and Measurement of Atherosclerotic Plaque. In: Mastorakis NE, Mladenov V, Bojkovic Z et al. (eds) PROCEEDINGS OF THE 13TH WSEAS INTERNATIONAL CONFERENCE ON COMPUTERS. WORLD SCIENTIFIC AND ENGINEERING ACAD AND SOC, AG LOANNOU THEOLOGOU 17-23, 15773 ZOGRAPHOU, ATHENS, GREECE, pp 303–306

[7] Licev L, Babiuch M, Farana R et al. (2013) Software Analysis of Mining Images for Objects Detection. ACTA MONTANISTICA SLOVACA 18(1): 59–66

[8] Blasiak S (2015) An analytical approach to heat transfer and thermal distortions in non-contacting face seals. International Journal of Heat and Mass Transfer 81: 90–102. doi: 10.1016/j.ijheatmasstransfer.2014.10.011

[9] Blasiak S, Laski PA, Takosoglu JE (2013) Parametric analysis of heat transfer in non-contacting face seals. International Journal of Heat and Mass Transfer 57(1): 22–31. doi: 10.1016/j.ijheatmasstransfer.2012.09.058